Article

Selective hydrogenolysis of glycerol to propylene glycol on supported Pd catalysts: Promoting effects of ZnO and mechanistic assessment of active PdZn alloy surfaces

Qianhui Sun, Shuai Wang, and Haichao Liu

ACS Catal., **Just Accepted Manuscript** • Publication Date (Web): 16 May 2017

Selective hydrogenolysis of glycerol to propylene glycol on supported Pd catalysts: Promoting effects of ZnO and mechanistic assessment of active PdZn alloy surfaces

Qianhui Sun,† *Shuai Wang,*† *and Haichao Liu**

Beijing National Laboratory for Molecular Sciences, State Key Laboratory for Structural Chemistry of Unstable and Stable Species, College of Chemistry and Molecular Engineering, Peking University, Beijing 100871, China

ABSTRACT:

Pd catalysts receive increasing attention for selective hydrogenolysis of glycerol to propylene glycol, because of their good hydrothermal stability and high selectivity for cleavage of C-O bonds over C-C bonds. Addition of Zn can facilitate glycerol hydrogenolysis to propylene glycol on Pd surface, but the promoting role of Zn, stability of the resulting active PdZn alloys and reaction mechanism remain largely unexplored. Here, we synthesized monoclinic zirconia-supported PdZn (PdZn/m-ZrO_2) catalysts via incipient wetness impregnation method. Glycerol hydrogenolysis turnover rates (normalized per surface Pd atom measured by H_2 chemisorption) and propylene glycol selectivity on these PdZn/m-ZrO_2 catalysts depended sensitively on their Zn/Pd molar ratios, and Zn leaching from the PdZn alloy phases led to deactivation of PdZn/m-ZrO_2. Such deactivation was efficiently inhibited when physical mixtures of Pd/m-ZrO_2 and ZnO were directly used in glycerol hydrogenolysis, leading to *in situ* formation of PdZn alloy layers on Pd surfaces with excellent stability and recyclability. Dependence of turnover rates on

glycerol and H_2 concentrations, combined with the primary kinetic isotope effects (k_H/k_D = 2.6 at 493 K), unveils the kinetically-relevant step of glycerol hydrogenolysis involving the α-C-H cleavage in 2,3-dihydroxypropanoxide intermediate to glyceraldehyde on PdZn alloys and Pd. Measured rate constants show that the transition state of α-C-H cleavage is more stable, due to the stronger oxophilicity of Zn, on PdZn alloys than on Pd, which thus facilitates α-C-H cleavage of the Zn-bound intermediate by adjacent Pd on PdZn alloys. Such synergy between Zn and Pd sites accounts for the observed superiority of PdZn alloys to Pd in glycerol hydrogenolysis.

KEYWORDS: selective hydrogenolysis, glycerol, propylene glycol, PdZn alloy, kinetics, H/D isotope effects

1. INTRODUCTION

Selective hydrogenolysis of glycerol to propylene glycol provides an economically viable route for conversion of glycerol by-products, in large surplus from biodiesel production, to value-added products.[1-6] A wide range of transition metals (e.g. Ru,[7-9] Rh,[10] Pt,[11] Pd,[12] Cu,[13-18] Co,[19,20] and Ni[21]) can catalyze this reaction, and have been intensively studied to date.[22,23] Previous studies reported that the selectivity to C-O cleavage over C-C cleavage, required for synthesis of propylene glycol in glycerol hydrogenolysis, follows an order of Ru < Rh < Pt < Pd < Cu, while their hydrogenolysis rates show a reverse order.[14, 24-26] In particular, Pd is selective to propylene glycol, similar to Cu, but with superior activity and hydrothermal stability,[12,26] which renders Pd-based catalysts potentially more favorable for the selective glycerol hydrogenolysis to propylene glycol.

Introduction of additional metals (e.g. Co,[12,27] Fe,[12,27] and Zn[28,29]) to monometallic Pd catalysts can modify the property of Pd surface and consequently improve its glycerol hydrogenolysis rate and selectivity to propylene glycol. Especially, great attention has been paid to bimetallic Pd-Zn catalysts, because of the readily formation of uniform PdZn alloys and their wide applications, not only in glycerol hydrogenolysis,[28,29] but also in other different reactions, such as methanol reforming [30-32] and water-gas shift reactions.[33,34] In particular, a high propylene glycol selectivity of 92.3% was obtained at 80.4% glycerol conversion for glycerol hydrogenolysis on a PdZn/ZnO@Al_2O_3 catalyst at 503 K and 3 MPa H_2.[29] The PdZn catalysts were mainly prepared via the reduction of dispersed Pd precursors on ZnO-based supports. However, the use of ZnO encounters two problems: (a) the Zn/Pd ratio of the PdZn alloys cannot be mediated, which is critical to the catalytic activity of the PdZn alloys;[34,35] (b) ZnO support is unstable in glycerol hydrogenolysis reactions because of its poor hydrothermal stability,[28] and thus needs to be stabilized by structural promoters (e.g. Al_2O_3).[29]

Glycerol hydrogenolysis to propylene glycol on metal surfaces in neutral and basic aqueous solutions involves glycerol dehydrogenation to glyceraldehyde, glyceraldehyde dehydration to 2-hydroxyacrylaldehyde, and sequential hydrogenations of 2-hydroxyacrylaldehyde to acetol and propylene glycol (Scheme 1).[2,14] The first dehydrogenation step has been widely proposed as a kinetically-relevant step on different metals, such as Ru, Rh, Pt, Pd, and Cu, based on the good correlations between their glycerol dehydrogenation activity and hydrogenolysis turnover rates,[8,26] and also on the independence of initial glycerol hydrogenolysis rates on H_2 pressures as observed with Cu-based catalysts.[14] However, kinetic and isotopic evidences for the glycerol hydrogenolysis mechanism on these metal catalysts are rare, and thus the kinetic relevance of the involved elementary steps remains still ambiguous. Such mechanistic details are clearly required

to further improve the efficacy of the metal catalysts, and for the specific case of the PdZn alloys, to elucidate the promoting effect of Zn on the Pd activity in glycerol hydrogenolysis.

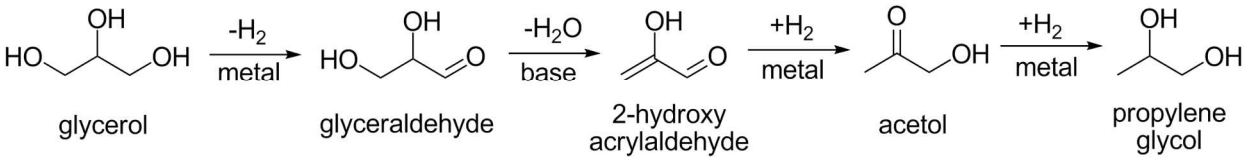

Scheme 1. Reaction route of glycerol hydrogenolysis to propylene glycol on metal catalysts in neutral and basic aqueous solutions.

In an attempt to address the aforementioned problem with the stability of the PdZn alloy phases, we herein prepare PdZn catalysts on hydrothermally-stable monoclinic ZrO_2 (m-ZrO_2) support via two different methods, i.e. incipient wetness impregnation of Pd/m-ZrO_2 with zinc acetate and physical mixing of Pd/m-ZrO_2 with ZnO. On these catalysts, reaction kinetic and isotopic studies are carried out to elucidate the reaction mechanism for glycerol hydrogenolysis. We find that for PdZn/m-ZrO_2 catalysts, the glycerol hydrogenolysis rate and propylene glycol selectivity sensitively depend on their Zn/Pd ratios. Active PdZn alloy phases can be readily formed *in situ* on m-ZrO_2 directly from physical mixtures of Pd/m-ZrO_2 and ZnO with excellent recyclability in glycerol conversion to propylene glycerol. Rigorous kinetic and isotopic assessment of the reaction pathways and mechanism shows that the α-C-H bond cleavage of glycerol on Pd/m-ZrO_2 and PdZn/m-ZrO_2 is the kinetically-relevant step in glycerol hydrogenolysis, which is facilitated by synergism between adjacent Pd and Zn sites on the PdZn alloys.

2. EXPERIMENTAL SECTION

2.1. Catalyst preparation. 1.0 wt% and 10 wt% Pd nanoparticles supported on monoclinic ZrO_2 (m-ZrO_2, 99%, Alfa Aesar) were prepared by incipient wetness impregnation, and were denoted as Pd/mZrO_2-1.0 and Pd/m-ZrO_2-10, respectively. A diluted HCl solution of $PdCl_2$

(A.R., Shenyang Research Institute of Nonferrous Metals) was added dropwise to m-ZrO_2. The resulting solids were treated in ambient air at 383 K overnight, heated to 823 K at 5 K min^{-1}, and then held at 823 K for 4 h in flowing air (40 mL min^{-1}). These samples (denoted as PdO/m-ZrO_2) were subsequently treated in flowing 20% H_2/N_2 (>99.99%, Beijing Huayuan, 40 mL min^{-1}) at 673 K (5 K min^{-1}) for 3 h. Pd dispersions for Pd/m-ZrO_2-1.0 and Pd/m-ZrO_2-10, estimated from H_2 chemisorption (described in Section 2.2), were 19.6% and 14.5%, respectively.

PdZn/m-ZrO_2 catalysts (denoted as PdZn/m-ZrO_2-x(y), where x represents the weight percentages for Pd loadings, and y represents the Zn/Pd molar ratio, $0 \leq y \leq 8.0$ when $x = 1.0$, and $0 \leq y \leq 2.0$ when $x = 10$) were prepared via incipient wetness impregnation of PdO/m-ZrO_2 samples with an aqueous solution of zinc acetate ($Zn(AcO)_2 \cdot 2H_2O$, 98%, Alfa Aesar). These samples were treated in ambient air at 383 K overnight, and then in flowing 20% H_2/N_2 (40 mL min^{-1}) at 773 K (5 K min^{-1}) for 3 h for the formation of PdZn alloys.[30] The compositions of these catalysts were measured by inductively coupled plasma-atomic emission spectrometry (ICP-AES, Teledyne Leeman Labs). H_2-chemisorption showed that Pd dispersions for the PdZn/m-ZrO_2 samples were similar to those of the Pd/m-ZrO_2 samples with the same Pd loadings.

2.2. Catalyst characterization. XRD patterns were recorded on a Rigaku D/MAX-2400 diffractometer in the 2θ range of 30-60°, using Cu $K\alpha_1$ radiation (λ = 1.5406 Å) operated at 40 kV and 100 mA. X-ray photoelectron spectra (XPS) were collected on an Axis Ultra spectrometer (Kratos Analytical Ltd.) using monochromatic Al Kα radiation (hv = 1486.6 eV) operated at 150 W; samples were treated in flowing 20% H_2/N_2 (40 mL min^{-1}) at 493 K for 2 h in a process chamber before the XPS characterization, in order to eliminate slow oxidation of the metal catalysts caused by the unavoidable exposure to ambient air. The binding energies were calibrated by referring to the Zr $3d_{5/2}$ signal of m-ZrO_2 (182.1 eV).[36] H_2-chemisorption

(Quantachrome Autosorb-1) was used to measure the dispersion of Pd for Pd/m-ZrO_2 and PdZn/m-ZrO_2 catalysts, assuming the chemisorption stoichiometry of 1/1 for H/Pd. Samples were treated in flowing 5% H_2/N_2 (>99.99%, Beijing Huayuan; 10 mL min^{-1}) at 673 K (5 K min^{-1}) for 2 h and evacuated at the same temperature for 12 h; H_2-chemisorption was performed at 373 K and within 10-50 kPa H_2.

2.3. Glycerol hydrogenolysis reactions. Catalytic reactions were carried out in a 100 mL Teflon-lined stainless steel autoclave with vigorous stirring at a speed of 700 rpm. A certain amount of glycerol (A.R., Beijing Chemical) was first added into the autoclave and diluted with deionized water to 50 g to prepare the glycerol solution with a certain mass concentration (e.g. 5 g glycerol and 45 g water for a 10 wt% glycerol solution). Pd-based catalysts (i.e. Pd/m-ZrO_2 and PdZn/m-ZrO_2), together with additives (e.g. ZnO (A.R.), MgO (A.R.), or $Zn(AcO)_2{\cdot}2H_2O$ (98%), all purchased from Alfa Aesar and used without further thermal treatments) in cases mentioned below, were then added to the glycerol aqueous solution. The autoclave was pressurized with H_2 (>99.99%, Beijing Huayuan) after fully purging out the air, and heated to the reaction temperature (463-513 K) monitored by a thermocouple inserted in the autoclave. The concentrations of glycerol and hydrogenolysis products were analyzed by high-performance liquid chromatography (HPLC; Shimadzu LC-20A) using a RID detector and an Alltech OA-1000 organic acid column (0.005 mol L^{-1} H_2SO_4 mobile phase, 0.6 mL min^{-1} flow rate, and 343 K oven temperature). Turnover rates ($mol_{glycerol}$ $(mol_{surface\text{-}Pd}{\cdot}ks)^{-1}$) were reported as molar glycerol conversion rates per mole of exposed Pd atoms estimated from the H_2-chemisorption data, as described in Section 2.2; product selectivities were reported on a carbon basis. For recycling tests, the used catalysts were washed three times with deionized water and three times with acetone, and then dried in a vacuum oven at ambient temperature before the next cycle.

Kinetic isotope effects for the glycerol hydrogenolysis on Pd-based catalysts were examined with deuterated glycerol-1,1,2,3,3-d_5 reactants (98 atom% D, Sigma-Aldrich), in which all H-atoms in the C-H bonds of glycerol were replaced by D-atoms. Glycerol hydrogenolysis rates and selectivities for glycerol-1,1,2,3,3-d_5 were measured using the protocols described above for the protium-form glycerol reactants.

3. RESULTS AND DISCUSSION

3.1. Turnover rates, selectivity, and stability of Pd/m-ZrO_2 and PdZn/m-ZrO_2 catalysts.

Hydrogenolysis of glycerol on Pd/m-ZrO_2 and PdZn/m-ZrO_2 catalysts dominantly forms C_3 (e.g. propylene glycol, acetol and 1-propanol) and C_2 (e.g. ethylene glycol) products via cleavage of C-O bonds and C-C bonds, respectively (Scheme 2). Examined for comparison, glycerol did not show detectable conversion on m-ZrO_2 support under the identical conditions, as reported previously,[26] consistent with the requirement of metal function for dehydrogenation of glycerol to glyceraldehyde as an initial step involved in glycerol hydrogenolysis in neutral aqueous solutions (Scheme 1). The selectivities of propylene glycol, acetol and 1-propanol on Pd/m-ZrO_2-10 (with 10 wt% Pd loading and Pd nanoparticles of 6.9 nm) at 493 K and 6.0 MPa H_2, were 78.5%, 7.8%, and 4.3%, respectively (Table 1), while the selectivity of ethylene glycol was 7.4% at ~20% glycerol conversion. The combined selectivity of the C_3 products reached 90.6%, reflecting the preferential cleavage of C-O bond over C-C bond for glycerol hydrogenolysis on Pd-based catalysts.[24] The high selectivities to the C_3 products (95.0%) were also obtained on Pd/m-ZrO_2-1.0 with a lower Pd loading (1.0 wt%) and smaller Pd nanoparticles (5.1 nm). The turnover rate on Pd/m-ZrO_2-1.0 was slightly lower than that on Pd/m-ZrO_2-10 (7.4 vs. 11.1

$mol_{glycerol}$ $(mol_{surface\text{-}Pd}{\cdot}ks)^{-1}$, Table 1), indicating that larger Pd particles are more active in glycerol hydrogenolysis, as also observed for Ru/m-ZrO_2 catalysts.[26]

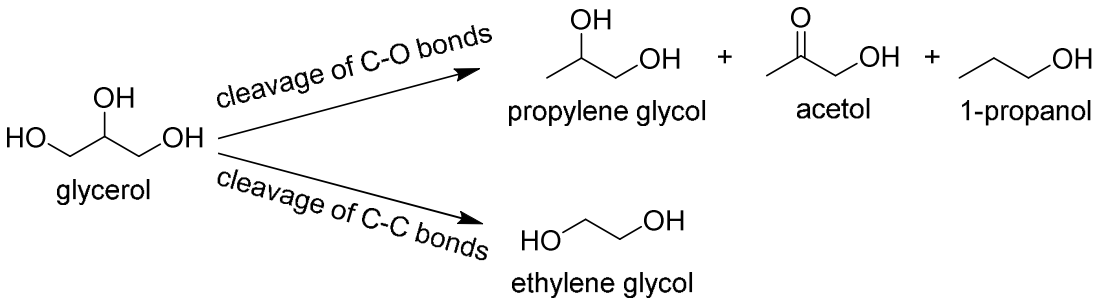

Scheme 2. Products of glycerol hydrogenolysis on Pd-based catalysts.

Table 1. Turnover rates and selectivities of glycerol hydrogenolysis on Pd/m-ZrO_2 and PdZn/m-ZrO_2 catalysts.[a]

Catalyst	Turnover rate ($mol_{glycerol}$ $(mol_{surface\text{-}Pd}{\cdot}ks)^{-1}$)	Selectivity (on a carbon basis, %)			
		Propylene glycol	Ethylene glycol	Acetol	1-Propanol
Pd/m-ZrO_2-10[b]	11.1	78.5	7.4	7.8	4.3
Pd/m-ZrO_2-1.0[b]	7.4	77.4	2.6	3.0	14.6
PdZn/m-ZrO_2-10(1.2)[c]	119.5	91.5	2.8	0.3	1.8
PdZn/m-ZrO_2-1.0(5.0)[c]	90.9	93.2	2.1	0.3	1.2
Pd/m-ZrO_2-1.0+ZnO[c]	90.2	94.1	2.5	0.8	2.5
Pd/m-ZrO_2-1.0+MgO[b]	7.0	80.7	8.8	4.9	1.5

[a]Reaction conditions: 493 K, 6.0 MPa H_2, 10 wt% glycerol in water, 1 g catalyst with a 1 wt% Pd loading or 0.1 g catalyst with a 10 wt% Pd loading; additive: 0.04 g ZnO or 0.2 g MgO. [b]20 h, ~20% glycerol conversion. [c]4 h, ~40% glycerol conversion.

Upon formation of PdZn alloy phases on the Pd/m-ZrO_2 catalysts, as described in Section 2.1, via treating them with impregnated $Zn(AcO)_2$ in flowing H_2 at 773 K, the glycerol hydrogenolysis rate and propylene glycol selectivity significantly increased, depending on Zn/Pd molar ratios. Figure 1 shows that the turnover rates on PdZn/m-ZrO_2-10(y) ($0 \leq y$ (Zn/Pd molar

ratio) ≤ 2.0; 493 K, 6.0 MPa H_2, 10 wt% glycerol aqueous solution henceforth) increased from 11.1 to 119.5 $mol_{glycerol}$ $(mol_{surface\text{-}Pd}{\cdot}ks)^{-1}$ with increasing the Zn/Pd ratio from 0 to 1.2, and then decreased to 50.9 $mol_{glycerol}$ $(mol_{surface\text{-}Pd}{\cdot}ks)^{-1}$ with a further increase of the Zn/Pd ratio to 2.0. Concurrently, the selectivity to propylene glycol increased from 78.5% to a maximum value of 91.5% with increasing the Zn/Pd ratio to 1.2, at the expense of the selectivities to acetol (7.8% vs. 0.3%), 1-propanol (4.3% vs. 1.8%), and ethylene glycol (7.4% vs. 2.8%) (Table 1). Similar effects of Zn/Pd ratios were also observed for PdZn/m-ZrO_2-1.0 in the range of 0-8.0 (Table 1 and Fig. S1 in Supporting Information (SI)). At the optimal Zn/Pd ratio of 5.0, the turnover rate and propylene glycol selectivity were increased to 90.9 $mol_{glycerol}$ $(mol_{surface\text{-}Pd}{\cdot}ks)^{-1}$ and 93.2%, respectively, showing the superiority of the PdZn alloys to monometallic Pd phase for the selective hydrogenolysis of glycerol to propylene glycol, irrespective of the Pd loadings (Table 1).

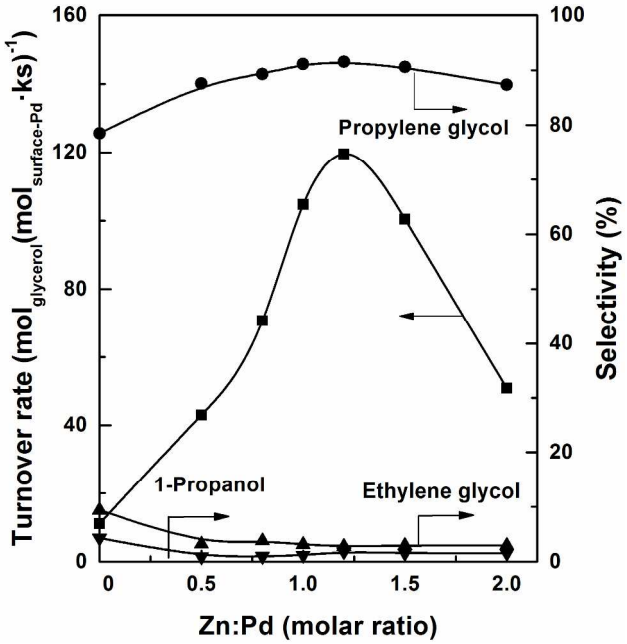

Figure 1. Effects of Zn/Pd molar ratio on turnover rates and selectivities in glycerol hydrogenolysis on PdZn/m-ZrO_2-10(y) ($0 \leq y$ (Zn/Pd molar ratio) ≤ 2.0, 0.1 g catalyst, 493 K, 6.0 MPa H_2, 4 h, 10 wt% aqueous glycerol solution). Acetol selectivities on all catalysts were below 2% and were not shown here.

The stability of the active PdZn alloys under glycerol hydrogenolysis conditions was examined using the PdZn/m-ZrO_2-10 sample with the optimal Zn/Pd molar ratio of 1.2. As shown in Figure 2, the hydrogenolysis turnover rates decreased from 119.5 to 35.3 $mol_{glycerol}$ $(mol_{surface\text{-}Pd} \cdot ks)^{-1}$ over seven consecutive runs (493 K, 6.0 MPa H_2, 4 h per run), in concomitance with a slight decrease of propylene glycol selectivity from 94.8% to 90.5%. Characterization of the catalyst by XRD and XPS showed no detectable change in the Pd particle size or oxidation state after the seventh run (as discussed below in Section 3.3). However, elemental analysis showed that the PdZn/m-ZrO_2-10 catalyst possessed a Zn/Pd molar ratio of only 0.68 after the seventh run, corresponding to a loss of 43% Zn during the recycling. The loss of Zn apparently led to the decrease of the turnover rate and propylene glycol selectivity, in line with the observed effects of Zn/Pd ratio on the activity and selectivity of PdZn alloys in glycerol hydrogenolysis (Fig. 1).

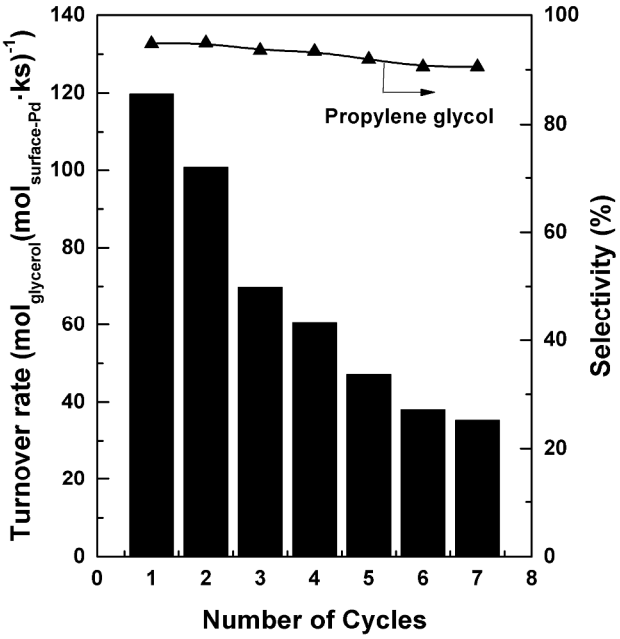

Figure 2. Turnover rates and selectivities to propylene glycol for seven consecutive cycles of glycerol hydrogenolysis on PdZn/m-ZrO_2-10(1.2) (0.1 g catalyst, 493 K, 6.0 MPa H_2, 4 h, 10 wt% aqueous glycerol solution).

We surmise that metallic Zn is readily oxidized by H_2O to form Zn^{2+} ions at hydrothermal conditions, and the dissolution of Zn^{2+} ions in the aqueous solution leads to the loss of Zn from the active PdZn alloys during glycerol hydrogenolysis reaction. This unstable nature of metallic Zn renders the PdZn alloys, even supported on stable m-ZrO_2 surface, impractical for reactions at such hydrothermal conditions of glycerol hydrogenolysis, in spite of their higher initial turnover rate and propylene glycol selectivity. Considering such nature of Zn and the consequent instability of PdZn alloys, in the next section, we report that direct use of physical mixtures of Pd/m-ZrO_2 and ZnO (denoted as Pd/m-ZrO_2+ZnO) leads to the *in situ* formation of active PdZn alloys on Pd surfaces under the glycerol hydrogenolysis conditions, and the presence of ZnO can provide Zn^{2+} ions to prevent the PdZn alloys from Zn leakage and consequently render them stable.

3.2. Turnover rates, selectivity, and stability of *in situ* formed PdZn alloys. ZnO was chosen here as a Zn^{2+} donor for PdZn alloys, because ZnO can partially hydrate to $Zn(OH)_2$, which then dissolves in hot water to from Zn^{2+} and OH^- ions. The concentration of OH^- ions derived from ZnO was limited by its solubility (0.3 mg mL^{-1} at 493 K, measured in glycerol hydrogenolysis conditions, Table S1, SI), and did not affect the glycerol hydrogenolysis turnover rate or propylene glycol selectivity, as evidenced by a control experiment using MgO (Table 1), which is more soluble than ZnO in H_2O.[37] Similar glycerol hydrogenolysis turnover rates (7.4 v.s 7.0 $mol_{glycerol}$ $(mol_{surface\text{-}Pd}{\cdot}ks)^{-1}$) and selectivities of propylene glycol (77.4% vs. 80.7%) were obtained on Pd/m-ZrO_2-1.0 and on its physical mixture with MgO (Table 1), although the use of MgO provided a higher concentration of OH^- ions than the case of ZnO. Therefore, ZnO can be regarded only as a source of Zn^{2+} ions in glycerol hydrogenolysis.

Figure 3 shows the glycerol hydrogenolysis turnover rates and selectivities as a function of ZnO amount on Pd/m-ZrO_2-1.0+ZnO. As the amount of ZnO increased from 0 to 0.04 g, the rates increased from 7.4 to 90.2 $mol_{glycerol}$ $(mol_{surface\text{-}Pd}{\cdot}ks)^{-1}$ at 493 K (Fig. 3), and then gradually decreased to 79.9 $mol_{glycerol}$ $(mol_{surface\text{-}Pd}{\cdot}ks)^{-1}$ as the ZnO amount further increased to 0.30 g. The selectivity to propylene glycol monotonically increased to 94.1%, which then remained almost constant upon addition of ZnO larger than 0.04 g (Fig. 3). Similar promoting effects were also observed in the control experiments when ZnO was replaced by soluble $Zn(AcO)_2$ salt (Fig. S2, SI), confirming that for Pd/m-ZrO_2+ZnO, it is the Zn^{2+} ions, derived from the dissolution of ZnO, to play the actual role in improving the turnover rate and selectivity of Pd/m-ZrO_2.

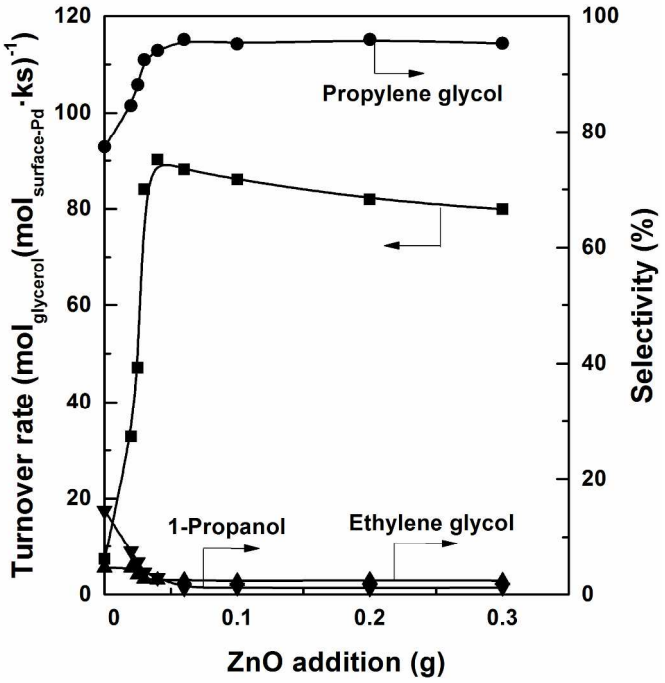

Figure 3. Turnover rates and selectivities in glycerol hydrogenolysis as a function of ZnO amount on Pd/m-ZrO_2-1.0 physically mixed with different amounts of ZnO (1 g Pd/m-ZrO_2-1.0, 493 K, 6.0 MPa H_2, 4 h, 10 wt% aqueous glycerol solution). Acetol selectivities on all catalysts were below 2% and were not shown here.

Such promoting effects of ZnO and Zn^{2+} ions resemble the observed effects of the Zn/Pd ratios for the PdZn/m-ZrO_2 catalysts (Figs. 1 and S1). For example, the maximum glycerol

hydrogenolysis turnover rate and the corresponding propylene glycol selectivity on Pd/m-ZrO_2-1.0+ZnO (0.04 g ZnO, Fig. 3) were close to those obtained from the optimal PdZn/m-ZrO_2-1.0(5.0) catalyst (Fig. S1) (90.2 vs. 90.9 $mol_{glycerol}$ $(mol_{surface\text{-}Pd}{\cdot}ks)^{-1}$, 94.1% vs. 93.2%, Table 1). Moreover, on the two catalysts, the apparent activation energies for glycerol hydrogenolysis at 463-513 K, estimated using the Arrhenius equation, were essentially same (123 ± 5 vs. 122 ± 3 kJ mol^{-1}, Fig. 4), which were lower than the value for Pd/m-ZrO_2-1.0 (135 ± 2 kJ mol^{-1}). These similarities between Pd/m-ZrO_2+ZnO and PdZn/m-ZrO_2 indicate the *in situ* formation of PdZn alloys on Pd/m-ZrO_2 in the presence of Zn^{2+} ions for Pd/m-ZrO_2+ZnO during the glycerol hydrogenolysis, as indeed confirmed by XRD and XPS in in the next section.

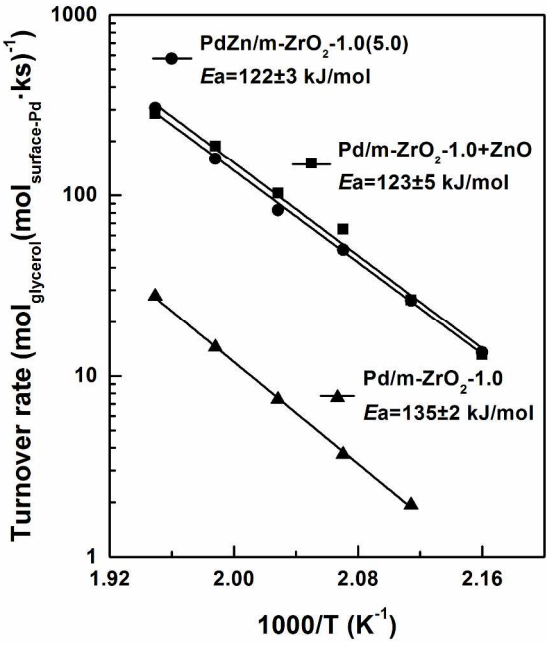

Figure 4. Effects of temperature on turnover rates in glycerol hydrogenolysis on Pd/m-ZrO_2-1.0+ZnO, PdZn/m-ZrO_2-1.0(5.0) and Pd/m-ZrO_2-1.0 (1 g catalyst, 6.0 MPa H_2, 10 wt% aqueous glycerol solution, ~20% glycerol conversion obtained by varying reaction time). Solid lines represent exponential regression fits.

It is noted that the physical mixtures of Pd/m-ZrO_2 and ZnO are stable and recyclable in glycerol hydrogenolysis. Representative results are shown in Figure 5. The turnover rate and propylene glycol selectivity on Pd/m-ZrO_2-1.0+ZnO remained constant for five consecutive runs

at 493 K and 6.0 MPa H_2, being 82.0-85.9 $mol_{glycerol}$ $(mol_{surface\text{-}Pd}{\cdot}ks)^{-1}$ and 94.1-93.7%, respectively, within the kinetic-controlled regime. Analysis of the filtrate after each run by ICP-AES showed no detectable leaching of Pd, while Zn^{2+} ions were detected in a concentration of 0.3 mg mL^{-1}, reflecting the solubility of ZnO at the reaction conditions. These constant rates and selectivities on Pd/m-ZrO_2+ZnO thus suggest that the presence of Zn^{2+} ions derived from ZnO stabilizes the active PdZn alloys during glycerol hydrogenolysis, which would otherwise undergo severe deactivation, as observed with PdZn/m-ZrO_2 (Fig. 2).

Such high stability of the physical mixtures of Pd/m-ZrO_2 and ZnO implies their potential as a facile source of the active PdZn alloys for practical application to the selective synthesis of propylene glycol from glycerol hydrogenolysis. Furthermore, even at 100% glycerol conversion, the propylene glycol selectivity remained as high as 91.8%, corresponding to a yield of 91.8%, on Pd/m-ZrO_2-1.0+ZnO (493 K, 6.0 MPa H_2; Fig. S3, SI).

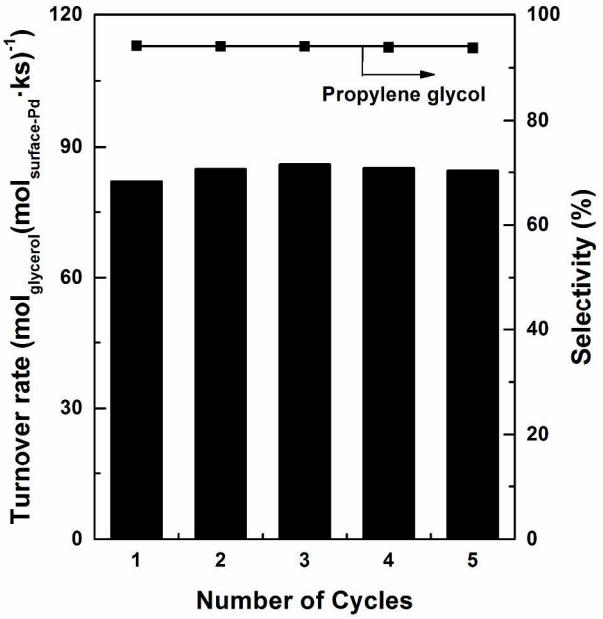

Figure 5. Turnover rates and selectivities to propylene glycol for five consecutive cycles of glycerol hydrogenolysis on Pd/m-ZrO_2-1.0+ZnO (1 g Pd/m-ZrO_2-1.0, 0.2 g ZnO, 493 K, 6.0 MPa H_2, 4 h, 10 wt% aqueous glycerol solution).

3.3. Structural characterization of Pd and PdZn catalysts before and after glycerol hydrogenolysis reaction. The monometallic Pd and PdZn alloy catalysts examined in this work were characterized by XRD and XPS, and the representative results are shown in Figures 6 and 7. Pd/m-ZrO_2-10 exhibits diffraction peaks at 40.1° and 46.7°, characteristic of metallic Pd, in addition to those of m-ZrO_2 support (Figs. 6a and b). For PdZn/m-ZrO_2-10(1.2), its diffraction peaks appeared at 41.2° and 44.1° (Fig. 6c), assigning to the (111) and (200) planes of PdZn alloy phases, respectively;[38] no diffractions for metallic Pd or any phases related to metallic Zn (e.g. 36.3° and 43.2°)[39] and ZnO (e.g. 31.8° and 36.3°)[40] were detected, indicating that PdZn alloys were solely present on m-ZrO_2 surface. XPS spectra confirmed the formation of PdZn alloys on m-ZrO_2. Relative to the binding energies of the Pd $3d_{3/2}$ and $3d_{5/2}$ signals for Pd/m-ZrO_2-10 (340.6 and 335.3 eV, Fig. 7a), these values for PdZn/m-ZrO_2-10(1.2) shifted by 0.7 eV to 341.3 and 336.0 eV, respectively (Fig. 7b), which reflects an electronic transfer from Pd to Zn in the PdZn alloys.[30] Similar XRD and XPS results (Figs. 6d and 7c) were obtained for PdZn/m-ZrO_2 after the glycerol hydrogenolysis reaction (493 K, 6.0 MPa H_2, 4h), suggesting that this catalyst still contained only PdZn alloys on m-ZrO_2, in spite of the detected leaching of the Zn component.

To confirm the formation of the PdZn alloys from the physical mixtures of Pd/m-ZrO_2-10 and ZnO during the glycerol hydrogenolysis reaction, XRD patterns were collected for Pd/m-ZrO_2-10 in the presence of ~0.60 mg mL^{-1} Zn^{2+} ions (using $Zn(AcO)_2{\cdot}2H_2O$ to mimic ZnO for simplicity) after the reaction. The pattern (Fig. 6e) shows only characteristic diffraction peaks of metallic Pd (at 2θ = 40.1° and 46.7°) with no any detectable peaks of PdZn alloys (at 2θ = 41.2° and 44.1°), similar to the pattern before the reaction (Fig. 6a), thus indicating that the bulk structure of Pd nanoparticles was not affected by Zn^{2+} ions during the reaction. Differently, the

corresponding XPS spectrum after the reaction (Fig. 7d) shows the binding energies of Pd $3d_{3/2}$ and $3d_{5/2}$ at 341.3 and 336.0 eV, respectively, identical to those for the PdZn alloys on PdZn/m-ZrO_2-10 (Fig. 7b). Taken together, these results suggest that the PdZn alloy layers are formed, most likely in the form of thin layers, via the reduction of Zn^{2+} ions on Pd surfaces during glycerol hydrogenolysis.

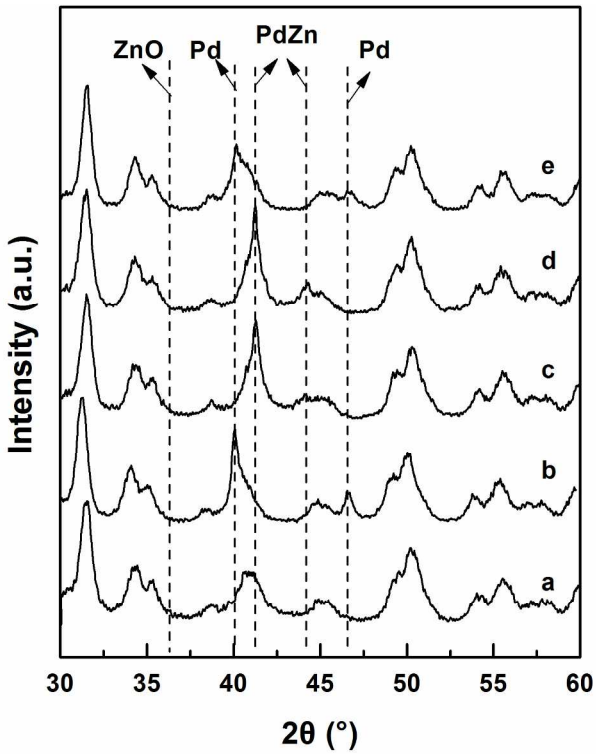

Figure 6. X-ray diffraction patterns of (a) m-ZrO_2, (b) Pd/m-ZrO_2-10 and (c) PdZn/m-ZrO_2-10(1.2) before glycerol hydrogenolysis reaction, and (d) PdZn/m-ZrO_2-10(1.2) and (e) a physical mixture of 0.1 g Pd/m-ZrO_2-10 and 0.1 g $Zn(AcO)_2{\cdot}2H_2O$ after glycerol hydrogenolysis reaction (493K, 6.0 MPa H_2, 4h, 10 wt% glycerol aqueous solution).

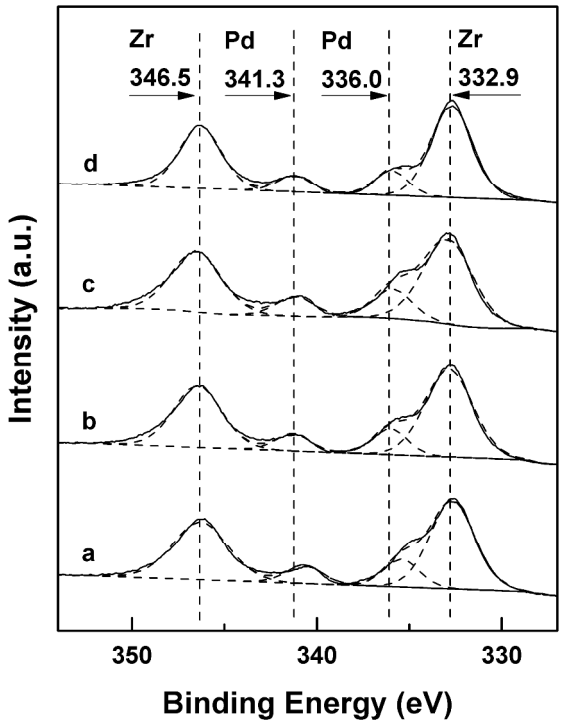

Figure 7. XPS spectra of Pd 3d and Zr 3p signals for (a) Pd/m-ZrO_2-10 and (b) PdZn/m-ZrO_2-10(1.2) before glycerol hydrogenolysis reaction, and (c) PdZn/m-ZrO_2-10(1.2) and (d) a physical mixture of 0.1 g Pd/m-ZrO_2-10 and 0.1 g $Zn(AcO)_2{\cdot}2H_2O$ after glycerol hydrogenolysis reaction (493K, 6.0 MPa H_2, 4h, 10 wt% glycerol aqueous solution).

3.4. Effects of glycerol and H_2 concentrations on turnover rates and the glycerol hydrogenolysis mechanism on PdZn alloy surfaces. The effects of concentrations of glycerol and H_2 on glycerol hydrogenolysis turnover rates and selectivities were examined at 493 K on PdZn alloys within kinetic-controlled regime (at ~20% glycerol conversions). The PdZn alloys were formed *in situ* on m-ZrO_2 directly from physical mixtures of Pd/m-ZrO_2 and ZnO under the glycerol hydrogenolysis conditions. The aforementioned high stability of the PdZn alloys allows rigorous kinetic and isotopic assessment of the reaction mechanism and the role of Zn in glycerol hydrogenolysis using Pd/m-ZrO_2+ZnO. As shown in Figure 8a, the glycerol hydrogenolysis rates increased almost linearly from 88.0 to 211 $mol_{glycerol}$ $(mol_{surface\text{-}Pd}{\cdot}ks)^{-1}$ with increasing glycerol concentration from 0.5 to 2.1 mol L^{-1} (i.e. 5-20 wt% aqueous solutions), and then approached a

constant value of 270 $mol_{glycerol}$ $(mol_{surface\text{-}Pd} \cdot ks)^{-1}$ at higher concentrations above 4.4 mol L^{-1} (i.e. 40 wt%). This rate dependence on the glycerol concentration indicates that the PdZn alloy surfaces are densely covered with the strongly adsorbed glycerol or alkoxide intermediates derived from the dissociation of hydroxyls in glycerol at high glycerol concentrations. However, propylene glycol selectivity was essentially unaffected by glycerol concentrations, which kept between 93.1-96.0% (Fig. S4a, SI).

As H_2 partial pressure increased from 1.0 to 7.0 MPa, the glycerol hydrogenolysis rates monotonically decreased from 298 to 138 $mol_{glycerol}$ $(mol_{surface\text{-}Pd} \cdot ks)^{-1}$ (Fig. 8b). The propylene glycol selectivity slightly varied in the range of 91.0-93.7% (Fig. S4b), except at the low H_2 pressure of 1.0 MPa, which led to a high acetol selectivity (13.5%) at the expense of propylene glycol (56.8%) because of the inefficient hydrogenation of acetol to propylene glycol. The strong inhibition of H_2 pressure on glycerol hydrogenolysis in such a broad range of H_2 pressures (1.0-7.0 MPa), taken together with weak adsorption of H_2 on PdZn alloys (shown below), indicates that glycerol hydrogenolysis on PdZn alloys is kinetically limited by glycerol dehydrogenation, which is thermodynamically unfavorable at high H_2 pressures, consistent with the kinetic isotope effects and reaction mechanism for glycerol hydrogenolysis, as discussed below.

The hydrogenolysis turnover rates of deuterated glycerol reactants (i.e. CD_2OH-CDOH-CD_2OH) were 1.6 times lower than those for the protium-form reactants (i.e. CH_2OH-CHOH-CH_2OH) at 493 K (Table 2), while their selectivities to propylene glycol (89.2% vs. 90.5%) and ethylene glycol (5.8% vs. 7.7%) remained essentially identical. This primary kinetic isotope effect (k_H/k_D = 2.6) on glycerol hydrogenolysis rates indicates that cleavage of C-H bonds is involved in the kinetically-relevant steps, which is consistent with regression fittings of the glycerol hydrogenolysis rates with mechanism-based rate equations, as discussed below.

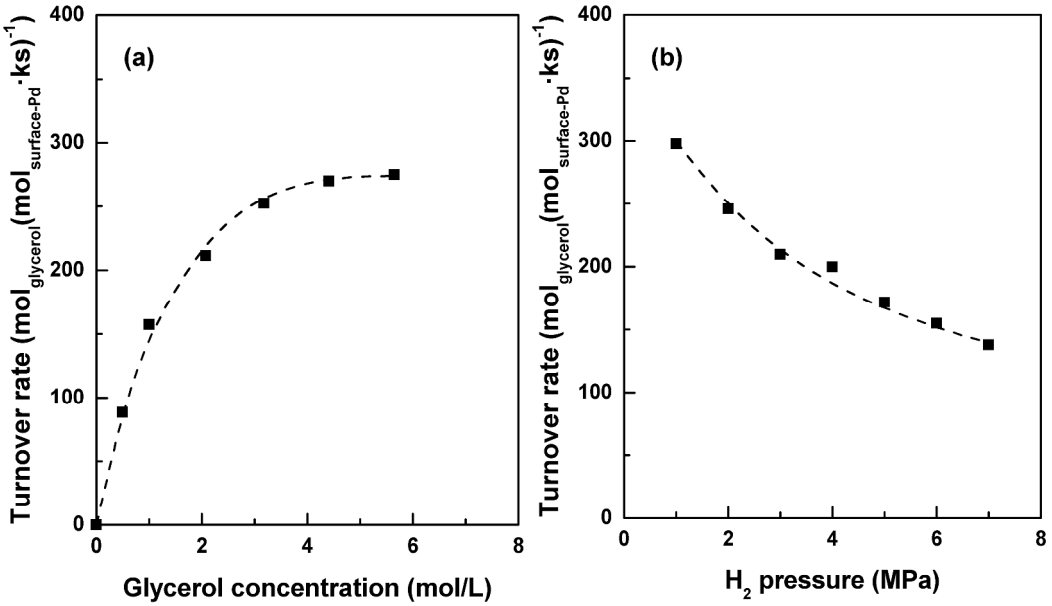

Figure 8. Effects of (a) glycerol concentration and (b) H_2 pressure on turnover rates in glycerol hydrogenolysis on Pd/m-ZrO_2-1.0+ZnO (1 g Pd/m-ZrO_2-1.0, 0.2 g ZnO, 493 K, ~20% glycerol conversion obtained by varying reaction time; (a) 6.0 MPa H_2; (b) 10 wt% aqueous glycerol solution). Dashed curves represent regressed fits to the functional form of Equation 1.

Table 2. Turnover rates and selectivities for glycerol and deuterated glycerol in hydrogenolysis reactions on Pd/m-ZrO_2-1.0+ZnO[a]

Reactant	Turnover rate	Selectivity (%)	
	($mol_{glycerol}(mol_{surface-Pd}\cdot ks)^{-1}$)	Propylene glycol	Ethylene glycol
$HOCH_2CH(OH)CH_2OH$	127	90.5	7.7
$HOCD_2CD(OH)CD_2OH$	48.7	89.2	5.8

[a]Reaction conditions: 0.3 g Pd/m-ZrO_2-1.0, 0.1 g ZnO, 493 K, 6.0 MPa H_2, 0.5 h, 0.5 g glycerol in 40 g water.

Glycerol hydrogenolysis on metal surfaces (such as Ru, Rh, Pt, Pd, and Cu) in neutral or basic aqueous solutions has been proved to occur via a dehydrogenation-dehydration-hydrogenation pathway.[14,26] A glycerol molecule adsorbed on metal surface first dissociates to form a bound alkoxide species (i.e. 2,3-dihydroxypropanoxide) and a H atom on two vicinal metal sites (Step 2, Scheme 3), which readily occurs even at modest temperatures.[41] An α-H atom in the bound alkoxide species is then abstracted by its adjacent vacant metal site to form

glyceraldehyde (Step 3, Scheme 3). Glyceraldehyde can desorb from the metal surfaces into aqueous solution (Step 5, Scheme 3) and dehydrate to 2-hydroxyacrylaldehyde with the aid of OH^- ions for the cleavage of a terminal C-O bond (Step 6, Scheme 3), which subsequently hydrogenates to acetol and propylene glycol. Alternatively, glyceraldehyde can undergo decarbonylation to ethylene glycol and CO (Step 7, Scheme 3). The CO molecule ultimately converts to CO_2 via water-gas shift reactions or to CH_4 with hydrogenolysis reactions.[26] In particular, α-C-H cleavage in 2,3-dihydroxypropanoxide to glyceraldehyde (Step 2, Scheme 3) has been proposed to be the kinetically-relevant step on different metal surfaces (i.e. Ru, Rh, Pt, Pd, and Cu),[14, 26] and the subsequent cleavage of C-O and C-C bonds (Steps 6 and 7, Scheme 3) determines the relative selectivities of propylene glycol and ethylene glycol.

1. Adsorption of glycerol on metal surface to form adsorbed glycerol species

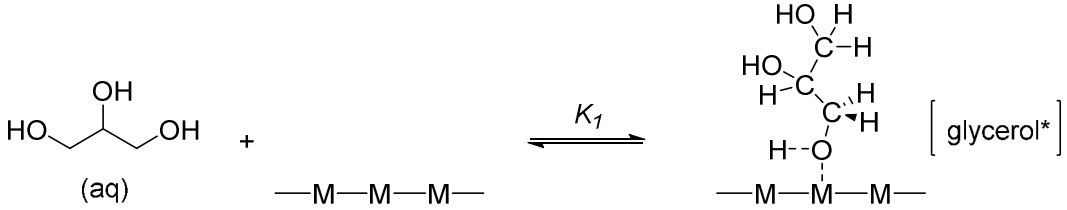

2. Dissociation of glycerol* to form a bound alkoxide species (2,3-dihydroxypropanoxide) and a bound H atom

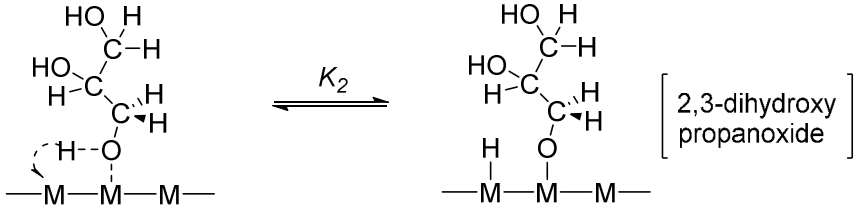

3. α-C-H cleavage of 2,3-dihydroxypropanoxide to form absorbed glyceraldehyde species

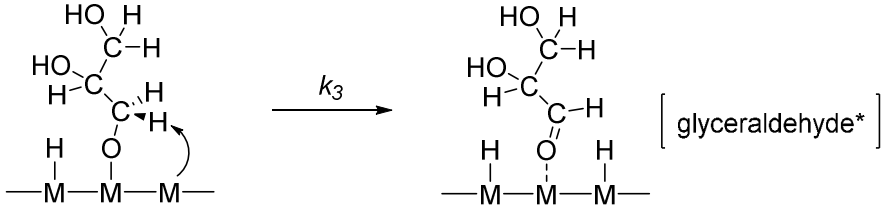

4. H_2 desorption

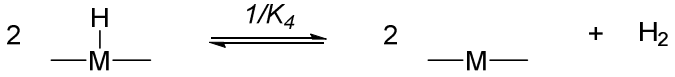

5. Glyceraldehyde desorption

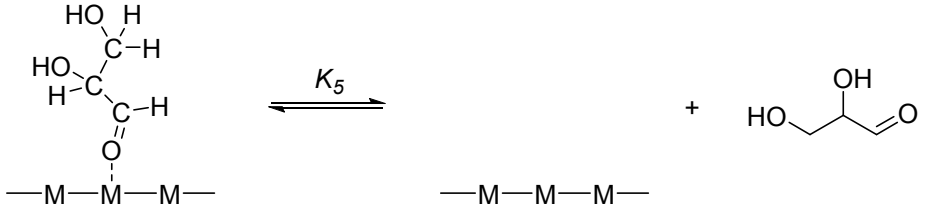

6. Dehydration of glyceraldehyde to form 2-hydroxyacrylaldehyde in H_2O

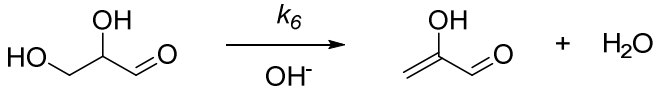

7. Decarbonylation of absorbed glyceraldehyde to form ethylene glycol and CO

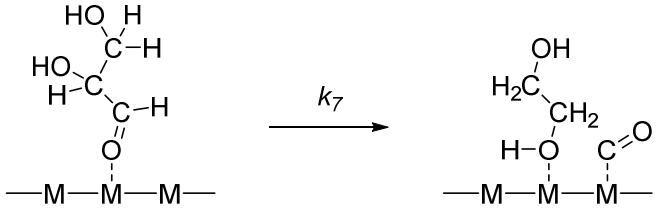

Scheme 3. Proposed sequence of elementary steps and associated kinetic constants and equilibrium constants for glycerol hydrogenolysis on metal surface.[26]

The kinetic relevance of the α-C-H cleavage in 2,3-dihydroxypropanoxide (Step 3, Scheme 3), taken together with the assumption of the quasi-equilibrated nature for Steps 1, 2, 4, and 5 in the proposed elementary steps (Scheme 3), gives the glycerol hydrogenolysis rate equation as

$$r = \frac{k_{C-H}[Gly][H_2]^{-\frac{1}{2}}}{\left(1 + K_1[Gly] + K_{Alk}[Gly][H_2]^{-\frac{1}{2}} + K_4^{\frac{1}{2}}[H_2]^{\frac{1}{2}}\right)^2} \quad (1)$$

Here, [Gly] is the activity of glycerol in water, [H_2] is the partial pressure of H_2 in gas phase; k_j and K_j are the respective kinetic constant and equilibrium constant for Step j in Scheme 3; k_{C-H} is the apparent kinetic constant for glycerol hydrogenolysis in aqueous phase:

$$k_{C-H} = k_3 K_1 K_2 K_4^{-\frac{1}{2}} \quad (2)$$

and K_{Alk} is the apparent equilibrium constant for the formation of bound 2,3-dihydroxypropanoxide from glycerol on metal surface:

$$K_{Alk} = K_1 K_2 K_4^{-\frac{1}{2}} \quad (3)$$

Equation 1 accurately described the rates measured in a broad range of reactant concentrations (5-50 wt% glycerol aqueous solutions, and 1.0-7.0 MPa H_2 in Fig. 8). A parity plot for the measured and predicted rates was shown in Figure 9a, and the corresponding regressed parameters of Equation 1 for the PdZn alloys were listed in Table 3. These excellent regression fits indicate that the proposed elementary steps in Scheme 3 reflect the mechanism of glycerol hydrogenolysis on PdZn alloys, and the glycerol hydrogenolysis rates are mediated by the α-C-H cleavage in glycerol to form glyceraldehyde intermediates, as also found on supported monometallic catalysts.[26] The Zn component in the PdZn alloys appears to stabilize the α-C-H cleavage transition states, leading to higher glycerol hydrogenolysis turnover rates. The regressed values for the relevant equilibrium constants in Equation 1 show that the $K_{Alk}[Gly][H_2]^{-\frac{1}{2}}$ term, which reflects the coverage of 2,3-dihydroxypropanoxide on metal surface, dominates the denominator (Table 3). This suggests that 2,3-dihydroxypropanoxide is the most abundant surface species (MASI) on the PdZn alloys in glycerol hydrogenolysis.

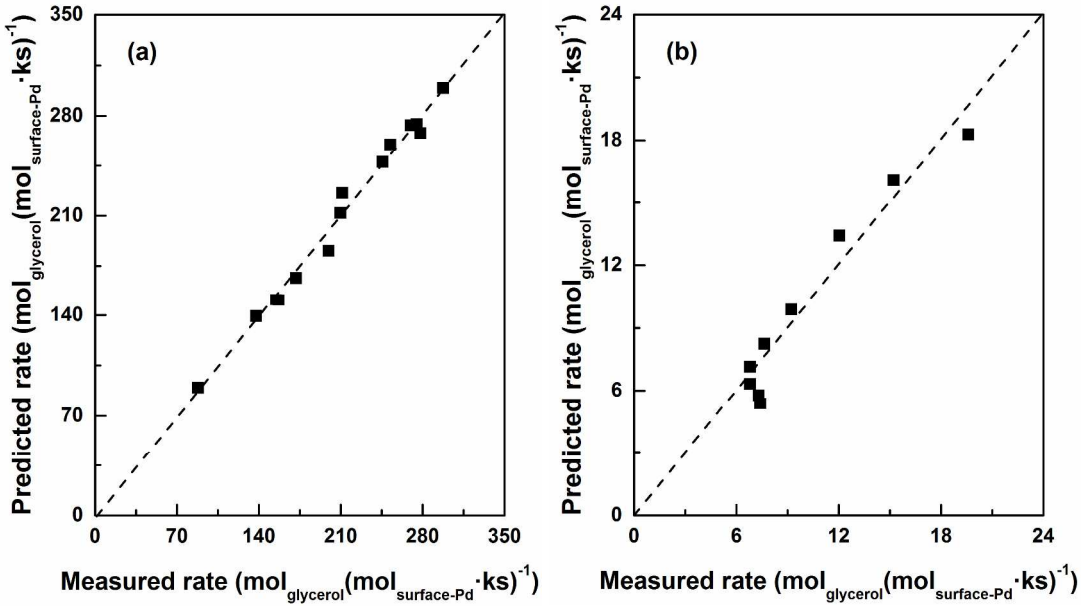

Figure 9. Parity plots for the measured and predicted rates of glycerol hydrogenolysis (Eq. (1)) on (a) a physical mixture of Pd/m-ZrO_2-1.0 and ZnO and (b) Pd/m-ZrO_2-1.0 with the regression-fitted parameters shown in Table 3.

Table 3. Regressed kinetic parameters for glycerol hydrogenolysis on Pd/m-ZrO_2-1.0+ZnO and Pd/m-ZrO_2-1.0 catalysts at 493 K.

Catalyst	k_{C-H} ((mol/L)$^{-1}$MPa$^{1/2}$s^{-1})	K_1 (mol/L)$^{-1}$	K_{Alk} ((mol/L)$^{-1}$ MPa$^{1/2}$)	$K_4^{\frac{1}{2}}$ (MPa)$^{-1/2}$
Pd/m-ZrO_2-1.0+ZnO	980 ± 70	< 0.01	0.65 ± 0.03	0.15 ± 0.02
Pd/m-ZrO_2-1.0	15 ± 2	< 0.01	0.15 ± 0.05	< 0.01

The dependence of glycerol hydrogenolysis rates on the concentrations of glycerol and H_2 was also examined for Pd/m-ZrO_2, in order to unveil the promoting effects of Zn on the Pd-catalyzed glycerol hydrogenolysis reactions. Figure 10 shows that the effects of the reactant concentrations on the glycerol hydrogenolysis rates resemble the trends observed on the PdZn alloys (Fig. 8). The glycerol hydrogenolysis rates on Pd/m-ZrO_2, however, were more sensitive to glycerol concentration and less sensitive to H_2 pressure, relative to those on the PdZn alloys, under the identical reaction conditions. As discussed for the PdZn alloys, the hydrogenolysis

rates on Pd/m-ZrO_2 were also accurately described by Equation 1 (Fig. 10), and the predicted rates agree excellently with the measured rates (Fig. 9b; the regressed parameters are shown in Table 3). These results indicate that the glycerol hydrogenolysis rates on Pd/m-ZrO_2 are also kinetically limited by the α-C-H cleavage in glycerol (Step 3, Scheme 3).

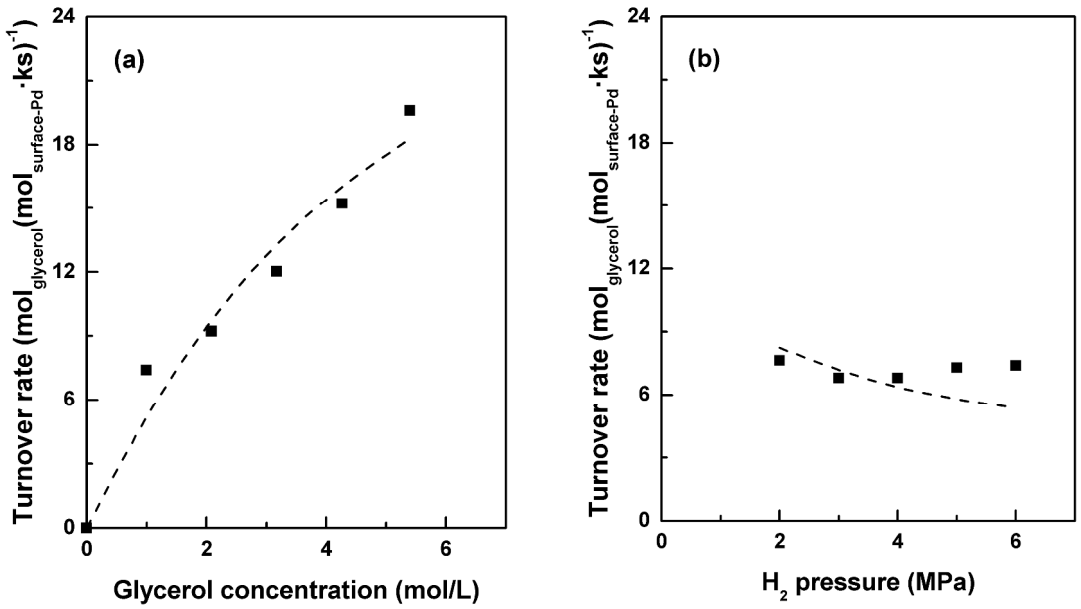

Figure 10. Effects of (a) glycerol concentration and (b) H_2 pressure on turnover rates in glycerol hydrogenolysis on Pd/m-ZrO_2-1.0 (493 K, ~20% glycerol conversion obtained by varying catalyst amount and reaction time; (a) 6.0 MPa H_2; (b) 10 wt% aqueous glycerol solution). Dashed curves represent regressed fits to the functional form of Equation 1.

The regressed value for k_{C-H} on the PdZn alloys (i.e. Pd/m-ZrO_2+ZnO) is over 60 times larger than that for Pd (i.e. Pd/m-ZrO_2) (980 ± 70 vs. 15 ± 2 (mol/L)$^{-1}$ MPa$^{1/2}$ s^{-1}, Table 3), consistent with the much higher hydrogenolysis turnover rates on the PdZn alloys (Figs. 1 and 3). As shown in Scheme 4, the k_{C-H} parameter reflects the difference ($\Delta G^{\ddagger}_{\text{C-H}}$) between the Gibbs free energy of the α-C-H cleavage transition state ($G^{\ddagger}_{\text{C-H}}$) and the sum of free energies of a glycerol molecule in aqueous solution (G_{Gly}) and of a bare metal surface (G_{M}):

$$\Delta G^{\ddagger}_{\text{C-H}} = G^{\ddagger}_{\text{C-H}} - G_{\text{Gly}} - G_{\text{M}} \quad (4)$$

The $\Delta G^{\ddagger}_{C\text{-}H}$ value for the PdZn alloys is lower than the value for Pd by 17 kJ mol^{-1} (i.e. $\Delta\Delta G^{\ddagger}_{C\text{-}H}$ in Scheme 4, 493 K), reflecting that the presence of Zn stabilizes the α-C-H cleavage transition states on the Pd surfaces. Such stabilization conferred by the PdZn alloys is also found for the adsorbed 2,3-dihydroxypropanoxide species, the precursor of the α-C-H cleavage transition state, as evidenced by the larger equilibrium constant for the formation of 2,3-dihydroxypropanoxide on PdZn than on Pd (K_{Alk}: 0.65 ± 0.03 vs 0.15 ± 0.03 (mol/L)$^{-1}$ MPa$^{1/2}$, 493 K, Table 3).

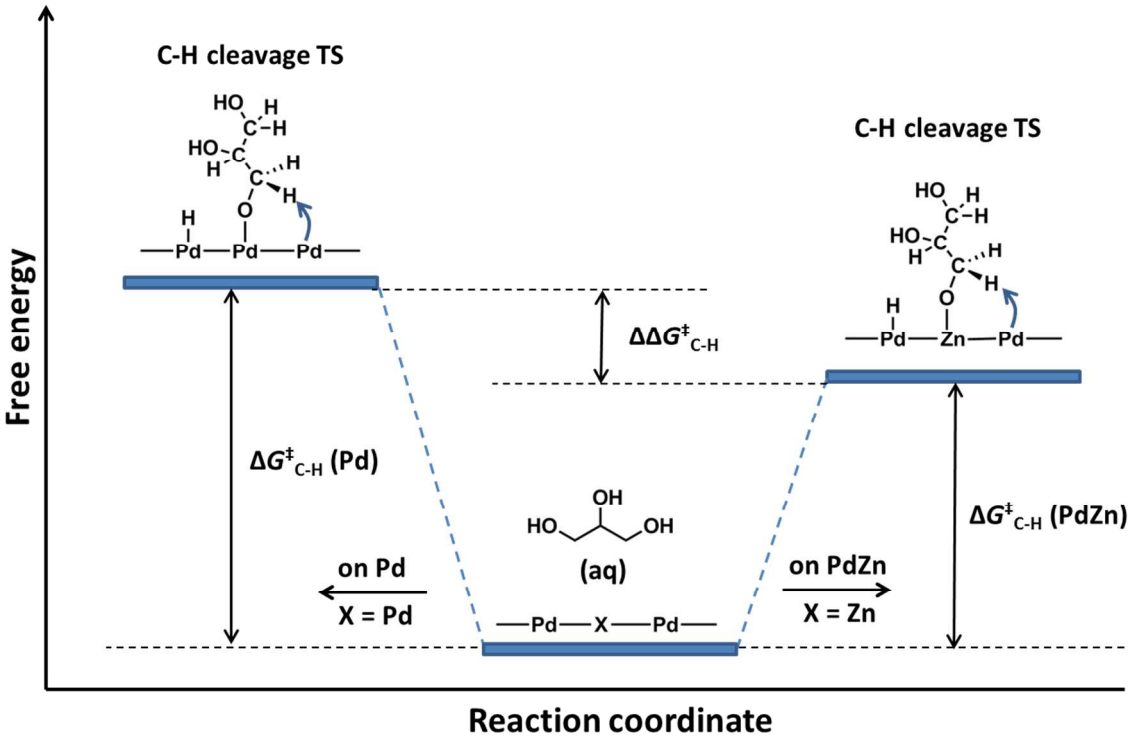

Scheme 4. Schematic reaction coordinate diagram of Gibbs free energy in glycerol hydrogenolysis on Pd and PdZn alloy surfaces. $\Delta G^{\ddagger}_{C\text{-}H}$ represents the experimentally measurable free energy barrier for glycerol hydrogenolysis.

The formation of PdZn alloys from the reduction of Zn^{2+} ions on the Pd surfaces can lead to a change in the electronic properties of the Pd sites (i.e. the known electronic effects of bimetallic catalysis[24]) and also to a collaboration between vicinal Pd and Zn sites in the kinetically-relevant α-C-H cleavage (i.e. the known synergistic effects of bimetallic catalysis[24]). Theoretical studies show that Pd in PdZn alloys exhibits a notably lower density of states at the Fermi level than

pure Pd, and resembles that for Cu.[42] Pure Cu catalysts, however, are much less reactive than Pd in glycerol hydrogenolysis.[14,26] Such comparison suggests that it is not the electronic effects induced by Zn on the PdZn alloy surfaces to contribute to the observed promoting effects on the hydrogenolysis turnover rates (Figs. 1 and 3). On the other hand, metallic Zn is more oxophilic than Pd,[43] and thus Zn is the preferred site to bind 2,3-dihydroxypropanoxide via the interaction between the Zn site and the terminal O atom in 2,3-dihydroxypropanoxide on the PdZn alloy surfaces, consistent with the higher measured K_{Alk} values on PdZn than on Pd (Table 3). The α-H atom in the 2,3-dihydroxypropanoxide species bound to a Zn site can be abstracted by a vicinal Pd site to form glyceraldehyde (Scheme 4). This synergy between Zn and Pd sites on the alloy surfaces would lead to stronger stability of the α-C-H cleavage transition state compared to pure Pd surfaces. The lower $\Delta G^{\ddagger}_{\text{C-H}}$ values measured on the PdZn alloy surfaces than on Pd thus indicate that the synergistic effects between the Zn and Pd sites account for the increased glycerol hydrogenolysis turnover rates on the PdZn alloy surfaces, as also found for other bimetallic catalysts (e.g. supported PtRe,[44] IrRe,[45] RhRe,[46] and RhMo[47]) in selective hydrogenolysis of other polyols and cyclic ethers, important reactions for upgrading of biomass-derived oxygenates into useful products.

4. CONCLUSIONS

Glycerol hydrogenolysis turnover rate and propylene glycol selectivity on PdZn/m-ZrO_2 are mediated by the Zn/Pd ratio of the PdZn alloy phases, both showing maximum values at moderate Zn/Pd ratios. These PdZn/m-ZrO_2 catalysts, however, tend to deactivate, because of the dissolution ability of metallic Zn and its consequent loss in the form of Zn^{2+} ions from the PdZn alloys in glycerol hydrogenolysis reactions. Such deactivation can be inhibited by addition of

Zn^{2+} donors (e.g. ZnO). The presence of the Zn^{2+} donors also leads to the *in situ* formation of active PdZn alloy layers on Pd/m-ZrO_2, which renders direct use of physical mixtures of Pd/m-ZrO_2 and ZnO as efficient and stable catalysts for glycerol hydrogenolysis to propylene glycol. Rigorous kinetic assessment, together with primary kinetic isotope effects, suggests that the cleavage of α-C-H bond in 2,3-dihydroxypropanoxide intermediate to form glyceraldehyde is the kinetically-relevant step in glycerol hydrogenolysis on the Pd and PdZn surfaces. The higher oxophilicity of Zn than Pd makes 2,3-dihydroxypropanoxide more stable on PdZn alloys than on Pd surfaces, and thus facilitates the abstraction of α-H atoms synergistically by adjacent Pd sites, leading to the observed superiority of the PdZn alloys to Pd.

ASSOCIATED CONTENT

Supporting Information

Effects of Zn/Pd ratio on rates and selectivities for PdZn/m-ZrO_2-1.0; Zn^{2+} concentration in filtrate after reaction as a function of the amount of ZnO additive; promoting effects of $Zn(AcO)_2 \cdot 2H_2O$ on rates and selectivities for Pd/m-ZrO_2-1.0; rates and selectivities as a function of glycerol conversion on Pd/m-ZrO_2+ZnO; and effects of glycerol and H_2 concentrations on the selectivity of glycerol hydrogenolysis on Pd/m-ZrO_2+ZnO

AUTHOR INFORMATION

Corresponding Author

*E-mail: hcliu@pku.edu.cn.

Author Contributions

†Q. Sun and S. Wang contributed equally to this work.

Notes

The authors declare no competing financial interest.

ACKNOWLEDGMENT

This work was supported by the National Natural Science Foundation of China (Grant Nos. 21690081, 21433001, 21373019) and the National Key Research and Development Program of China (Grant No.2016YFB0701100).

REFERENCES

(1) Gilkey, M. J.; Xu, B. *ACS Catal.* **2016**, 6, 1420-1436.

(2) Wang, Y. L.; Zhou, J. X.; Guo, X. W. *RSC Adv.* **2015**, 5, 74611-74628.

(3) Corma, A.; Iborra, S.; Velty, A. *Chem. Rev.* **2007**, 107, 2411-2502.

(4) Katryniok, B.; Paul, S.; Dumeignil, F. *ACS Catal.* **2013**, 3, 1819-1834.

(5) Nakagawa, Y.; Tomishige, K. *Catal. Sci. Technol.* **2011**, 1, 179-190.

(6) Hejna, A.; Kosmela, P.; Formela, K.; Piszczyk, Ł.; Haponiuk, J. T. *Renewable Sustainable Energy Rev.* **2016**, 66, 449-475.

(7) Miyazawa, T.; Kusunoki, Y.; Kunimori, K.; Tomishige, K. *J. Catal.* **2006**, 240, 213-221.

(8) Maris, E. P.; Davis, R. J. *J. Catal.* **2007**, 249, 328-337.

(9) Feng, J.; Wang, J. B.; Zhou, Y. F.; Fu, H. Y.; Chen, H.; Li, X. J. *Chem. Lett.* **2007**, 36, 1274-1275.

(10) Shinmi, Y.; Koso, S.; Kubota, T.; Nakagawa, Y.; Tomishige, K. *Appl. Catal., B* **2010**, 94, 318-326.

(11) Priya, S. S.; Kumar, V. P.; Kantam, M. L.; Bhargava, S. K.; Chary, K. V. R. *Catal. Lett.* **2014**, 144, 2129-2143.

(12) Musolino, M. G.; Scarpino, L. A.; Mauriello, F.; Pietropaolo, R. *ChemSusChem* **2011**, 4, 1143-1150.

(13) Wang, S.; Liu, H. C. *Catal. Lett.* **2007**, 117, 62-67.

(14) Wang, S; Zhang, Y. C.; Liu, H. C. *Chem. Asian J.* **2010**, 5, 1100-1111.

(15) Huang, Z. W.; Cui, F.; Kang, H. X.; Chen, J.; Zhang, X. Z.; Xia, C. G. *Chem. Mater.* **2008**, 20, 5090-5099.

(16) Huang, Z. W.; Cui, F.; Xue, J. J.; Zuo, J. L.; Chen, J.; Xia, C. G. *Catal. Today* **2012**, 183, 42-51.

(17) Xia, S. X.; Zheng, L. P.; Wang, L. N.; Chen, P.; Hou, Z. Y. *RSC Adv.* **2013**, 3, 16569-16576.

(18) Zheng, L. P.; Li, X. W.; Du, W. C.; Shi, D. W.; Ning, W. S.; Lu, X. Y.; Hou, Z. Y. *Appl. Catal., B* **2017**, 203, 146-153.

(19) Guo, X. H.; Li, Y.; Shi, R. J.; Liu, Q. Y.; Zhan, E. S.; Shen, W. J. *Appl. Catal., A* **2009**, 371, 108-113.

(20) Guo, X. H.; Li, Y.; Song, W.; Shen, W. J. *Catal. Lett.* **2011**, 141, 1458-1463.

(21) van Ryneveld, E.; Mahomed, A. S.; van Heerden, P. S.; Green, M. J.; Friedrich, H. B. *Green Chem.* **2011**, 13, 1819-1827.

(22) Sun, D.; Yamada, Y.; Sato, S.; Ueda, W. *Appl. Catal., B* **2016**, 193, 75-92.

(23) Nanda, M. R.; Yuan, Z. S.; Qin, W. S.; Xu, C. B. *Catal. Rev.: Sci. Eng.* **2016**, 58, 309-336.

(24) Alonso, D. M.; Wettstein, S. G.; Dumesic, J. A. *Chem. Soc. Rev.* **2012**, 41, 8075-8098.

(25) van Ryneveld, E.; Mahomed, A. S.; van Heerden, P. S.; Friedrich, H. B. *Catal. Lett.* **2011**, 141, 958-967.

(26) Wang, S.; Yin, K. H.; Zhang, Y. C.; Liu, H. C. *ACS Catal.* **2013**, 3, 2112-2121.

(27) Musolino, M. G.; Scarpino, L. A.; Mauriello, F.; Pietropaolo, R. *Green Chem.* **2009**, 11, 1511-1513.

(28) Li, X.; Zhang, C.; Cheng, H.; Lin, W.; Chang, P.; Zhang, B.; Wu, Q.; Yu, Y.; Zhao, F. *ChemCatChem* **2015**, 7, 1322-1328.

(29) Li, X.; Zhang, B.; Wu, Q.; Zhang, C.; Yu, Y.; Li, Y.; Lin, W.; Cheng, H.; Zhao, F. *J. Catal.* **2016**, 337, 284-292.

(30) Iwasa, N.; Takezawa, N. *Top. Catal.* **2003**, 22, 215-224.

(31) Rameshan, C.; Stadlmayr, W.; Weilach, C.; Penner, S.; Lorenz, H.; Hävecker, M.; Blume, R.; Rocha, T.; Teschner, D.; Knop-Gericke, A.; Schlögl, R.; Memmel, N.; Zemlyanov, D.; Rupprechter, G.; Klötzer, B. *Angew. Chem., Int. Ed.* **2010**, 49, 3224-3227.

(32) Friedrich, M.; Penner, S.; Heggen, M.; Armbrüster, M. *Angew. Chem., Int. Ed.* **2013**, 52, 4389-4392.

(33) Bollmann, L.; Ratts, J. L.; Joshi, A. M.; Williams, W. D.; Pazmino, J.; Joshi, Y. V.; Miller, J. T.; Kropf, A. J.; Delgass, W. N.; Ribeiro, F. H. *J. Catal.* **2008**, 257, 43-54.

(34) Dagle, R. A.; Platon, A.; Palo, D. R.; Datye, A. K.; Vohs, J. M.; Wang, Y. *Appl. Catal., A* **2008**, 342, 63-68.

(35) Neyman, K. M.; Lim, K. H.; Chen, Z. X.; Moskaleva, L. V.; Bayer, A.; Reindl, A.; Borgmann, D.; Denecke, R.; Steinruck, H. P.; Rosch, N. *Phys. Chem. Chem. Phys.* **2007**, 9, 3470-3482.

(36) Damyanova, S.; Grange, P.; Delmon, B. *J. Catal.* **1997**, 168, 421-430.

(37) Parks, G. A. *Chem. Rev.* **1965**, 65, 177-198.

(38) Tew, M. W.; Emerich, H.; van Bokhoven, J. A. *J. Phys. Chem. C* **2011**, 115, 8457-8465.

(39) Iwasa, N.; Mayanagi, T.; Masuda, S.; Takezawa, N. *React. Kinet. Catal. Lett.* **2000**, 69, 355-360.

(40) Ong, B. S.; Li, C.; Li, Y.; Wu, Y.; Loutfy, R. *J. Am. Chem. Soc.* **2007**, 129, 2750-2751.

(41) Davis, S. E.; Ide, M. S.; Davis, R. J. *Green Chem.* **2013**, 15, 17-45.

(42) Chen, Z. X.; Neyman, K. M.; Gordienko, A. B.; Rösch, N. *Phys. Rev. B* **2003**, 68, art. no. 075417.

(43) Johnson, R. S.; DeLaRiva, A.; Ashbacher, V.; Halevi, B.; Villanueva, C. J.; Smith, G. K.; Lin, S.; Datye, A. K.; Guo, H. *Phys. Chem. Chem. Phys.* **2013**, 15, 7768-7776.

(44) Falcone, D. D.; Hack, J. H.; Klyushin, A. Y.; Knop-Gericke, A.; Schlögl, R.; Davis, R. J. *ACS Catal.* **2015**, 5, 5679-5695.

(45) Amada, Y.; Shinmi, Y.; Koso, S.; Kubota, T.; Nakagawa, Y.; Tomishige, K. *Appl. Catal., B* **2011**, 105, 117-127.

(46) Chia, M.; Pagan-Torres, Y. J.; Hibbitts, D.; Tan, Q. H.; Pham, H. N.; Datye, A. K.; Neurock, M.; Davis, R. J.; Dumesic, J. A. *J. Am. Chem. Soc.* **2011**, 133, 12675-12689.

(47) Koso, S.; Ueda, N.; Shinmi, Y.; Okumura, K.; Kizuka, T.; Tomishige, K. *J. Catal.* **2009**, 267, 89-92.

TOC Graphic

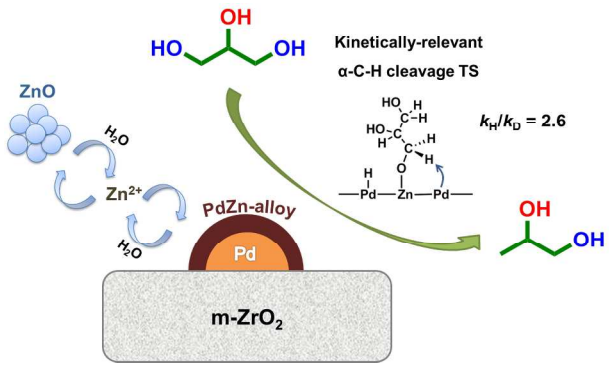
OH
HO
OH
Kinetically-relevant
α-C-H cleavage TS
k_H/k_D = 2.6
ZnO
H_2O
Zn^{2+}
H_2O
PdZn-alloy
Pd
m-ZrO_2
OH
OH